REGULAR ARTICLE

blood advances

Follicular lymphoma t(14;18)-negative is genetically a heterogeneous disease

Dominik Nann,[1,*] Joan Enric Ramis-Zaldivar,[2,3,*] Inga Müller,[1] Blanca Gonzalez-Farre,[2,3] Janine Schmidt,[1] Caoimhe Egan,[4] Julia Salmeron-Villalobos,[2,3] Guillem Clot,[2,3] Sven Mattern,[1] Franziska Otto,[1] Barbara Mankel,[1] Dolors Colomer,[2,3] Olga Balagué,[2,3] Vanessa Szablewski,[5] Carmen Lome-Maldonado,[6] Lorenzo Leoncini,[7] Stefan Dojcinov,[8] Andreas Chott,[9] Christiane Copie-Bergman,[10] Irina Bonzheim,[1] Falko Fend,[1] Elaine S. Jaffe,[4] Elias Campo,[2,3] Itziar Salaverria,[2,3,§] and Leticia Quintanilla-Martinez[1,§]

[1]Institute of Pathology and Neuropathology, Eberhard Karls University of Tübingen–Comprehensive Cancer Center, University Hospital Tübingen, Tübingen, Germany; [2]Hematopathology Unit, Hospital Clínic, Institut d'Investigacions Biomèdiques August Pi i Sunyer (IDIBAPS), Barcelona, Spain; [3]Centro de Investigación Biomédica en Red de Cáncer (CIBERONC), Madrid, Spain; [4]Hematopathology Section, Laboratory of Pathology, National Cancer Institute, National Institutes of Health, Bethesda, MD; [5]Department of Pathology, Montpellier University Hospital, Montpellier, France; [6]Department of Pathology, Instituto Nacional de Cancerologia, Mexico City, Mexico; [7]Section of Pathology, Department of Medical Biotechnology, University of Siena, Siena, Italy; [8]Department of Pathology, All Wales Lymphoma Panel, University Hospital of Wales, Cardiff, United Kingdom; [9]Institute of Pathology and Microbiology, Wilheminenspital, Vienna, Austria; and [10]Department of Pathology, Henri Mondor Hospital, Assistance Publique–Hôpitaux de Paris, INSERM U955, Université Paris Est, Creteil, France

Key Points

- t(14;18)$^-$ FL is genetically distinct from t(14;18)$^+$ FL, NMZL, and PTFL.
- *STAT6* mutations are frequent and co-occur with *TNFRSF14* and/or *CREBBP* alterations, revealing alternative oncogenic pathways.

Fifty-five cases of t(14;18)$^-$ follicular lymphoma (FL) were genetically characterized by targeted sequencing and copy number (CN) arrays. t(14;18)$^-$ FL predominated in women (M/F 1:2); patients often presented during early clinical stages (71%), and had excellent prognoses. Overall, t(14;18)$^-$ FL displayed CN alterations (CNAs) and gene mutations carried by conventional t(14;18)$^+$ FL (cFL), but with different frequencies. The most frequently mutated gene was *STAT6* (57%) followed by *CREBBP* (49%), *TNFRSF14* (39%), and *KMT2D* (27%). t(14;18)$^-$ FL showed significantly more *STAT6* mutations and lacked *MYD88*, *NOTCH2*, *MEF2B*, and *MAP2K1* mutations compared with cFL, nodal marginal zone lymphoma (NMZL), and pediatric-type FL (PTFL). We identified 2 molecular clusters. Cluster A was characterized by *TNFRSF14* mutations/1p36 alterations (96%) and frequent mutations in epigenetic regulators, with recurrent loss of 6q21-24 sharing many features with cFL. Cluster B showed few genetic alterations; however, a subgroup with *STAT6* mutations concurrent with *CREBBP* mutations/16p alterations without *TNFRSF14* and *EZH2* mutations was noted (65%). These 2 molecular clusters did not distinguish cases by inguinal localization, growth pattern, or presence of *STAT6* mutations. *BCL6* rearrangements were demonstrated in 10 of 45 (22%) cases and did not cluster together. Cases with predominantly inguinal presentation (20 of 50; 40%) had a higher frequency of diffuse growth pattern, *STAT6* mutations, CD23 expression, and a lower number of CNAs, in comparison with noninguinal cases (5.1 vs 9.1 alterations per case; $P < .05$). *STAT6* mutations showed a positive correlation with CD23 expression ($P < .001$). In summary, t(14;18)$^-$ FL is genetically a heterogeneous disorder with features that differ from cFL, NMZL, and PTFL.

Introduction

The genetic hallmark of conventional follicular lymphoma (cFL) is the chromosomal translocation t(14;18)(q32;q21) present in ~85% to 90% of cases, resulting in the constitutive overexpression of the

Submitted 14 July 2020; accepted 5 October 2020; published online 19 November 2020. DOI 10.1182/bloodadvances.2020002944.

*D.N. and J.E.R.-Z. contributed equally to this study.

§I.S. and L.Q-M. contributed equally to this study as senior authors.

All copy number array files have been deposited in the Gene Expression Omnibus database (accession number GSE80103). The sequencing data are deposited in the European Nucleotide Archive (accession number PRJEB38853).

The full-text version of this article contains a data supplement.

antiapoptotic protein BCL2.[1] In recent years, the genetic landscape of cFL has been characterized comprehensively, revealing that germinal center (GC)–derived lymphomas carry frequent mutations in histone-modifying genes.[2-5] The histone methyltransferases *KMT2D* and *EZH2*; the histone acetyltransferases *CREBBP*, *EP300*, and *MEF2B*; and the tumor necrosis factor receptor *TNFRSF14* are the most commonly mutated genes. cFL is also characterized by recurrent gains in the chromosomal regions 1q, 2p15, 7, 8q, 12q, 18p, and 18q, as well as losses in 1p36, 3q, 6q, 9p, 10q, 11q, 13q, and 17p.[6-8] Sites of recurrent copy number neutral–loss of heterozygosity (CNN-LOH) have been detected on 6p, 16p, 12q, 1p36, 10q, and 6q.[9] Interestingly, *CREBBP* and *TNFRSF14* are also affected by frequent deletions or CNN-LOH alterations that produce biallelic inactivation in a considerable number of cases (15% and 23%, respectively).[2,5]

FL t(14;18)$^-$ comprises 10% to 15% of all FL cases. Although BCL2 staining is a standard diagnostic procedure, it is not a perfect surrogate marker for the translocation, given that BCL2 protein is also expressed in a subset of t(14;18)$^-$ FL.[6,10,11] Furthermore, apparent lack of BCL2 expression can be observed in some FL with t(14;18) translocation related to altering of antibody binding by mutations.[12] Genetically, t(14;18)$^-$ FL is less well characterized, and its pathogenesis is largely unknown. A gene expression profiling study comparing t(14;18)$^-$ and t(14;18)$^+$ FLs showed signatures that point to subtle differences in the developmental stages of the neoplastic B cells, the usage of divergent oncogenic pathways, and the composition of the microenvironment.[6] Specifically, GCB-cell signatures were enriched in t(14;18)$^+$ FL, whereas ABC-like and post-GCB signatures were found to be overexpressed in t(14;18)$^-$ FL. Notably, t(14;18)$^-$ FLs showed evidence of ongoing somatic hypermutation, a feature of GCB-cells. It was therefore suggested that a subset of t(14;18)$^-$ FL may show the phenotype of a late GCB cell that has not yet exited the GC stage of differentiation. This latter observation was supported by a specific micro-RNA expression profile.[13]

A subset of t(14;18)$^-$ FLs shows a rearrangement affecting chromosomal band 3q27, which results in the deregulation of BCL6 expression.[14] *BCL6* translocation has been reported in grade 3B FLs (44%), which are more closely biologically related to diffuse large B-cell lymphoma than to other FLs.[15,16] Nevertheless, the frequency of t(3;14)(q27;q32) is also high (22%) in t(14;18)$^-$ FL grades 1 and 2,[17,18] suggesting an important role for *BCL6* in a subgroup of t(14;18)$^-$ FL.[19]

A group of t(14;18)$^-$ FL with a predominantly diffuse growth pattern and 1p36 chromosomal deletion was described by Katzenberger et al.[20] These cases were characterized by expression of CD23 and frequent loss of CD10 expression. Clinically, inguinal presentation predominates with early clinical stages (stages I and II) at diagnosis. Recently, it has been shown that these cases have frequent mutations of *STAT6*, *CREBBP*, *KMT2D*, and *TNFRSF14* genes; whether these cases represent a distinct subgroup within FL is as yet not clear.[21,22]

The diagnosis of t(14;18)$^-$ FL cases is difficult, and the differential diagnosis with reactive conditions, nodal marginal zone lymphomas (NMZLs)[23,24] and pediatric-type FL (PTFL) is challenging.[25-27] Because previous studies on t(14;18)$^-$ FL have included relatively few cases,[21,22] most of which showed BCL2 expression, we sought in this study to characterize the genetic profile of a large cohort of t(14;18)$^-$ FL, mostly without BCL2 expression, to identify specific genetic characteristics and correlate them with morphology, immunophenotype, and clinical features.

Material and methods

Lymphoma samples and clinical data

Fifty-five cases of t(14;18)$^-$ nodal FL, grades 1 to 3A were collected from the University of Tübingen (Germany), National Cancer Institute, National Institutes of Health (Bethesda, MD), Hospital Clinic (Barcelona, Spain), Hospital Henri-Mondor (Creteil, France), Wilheminenspital (Vienna, Austria), University Hospital of Wales (Cardiff, United Kingdom), and University of Siena (Italy). The cases were reviewed by 5 of the authors (E.C., B.G.F., O.B., E.S.J., and L.Q.-M.), according to the criteria of the 2017 World Health Organization classification.[1] Ten of the cases have been published.[26] All cases had at least 50% tumor cells. The morphology, growth pattern, cytology, and immunohistochemical staining for CD20, CD79a, BCL6, BCL2, CD10, CD3, MIB1, and CD23 were evaluated in formalin-fixed, paraffin-embedded (FFPE) tissue sections. The study was conducted in accordance with the Declaration of Helsinki and was approved by the local Ethics Review Committee and the institutional review board panels of the contributing institutions (UKT 348/2020B0).

DNA extraction and clonality analysis

DNA was extracted from FFPE tissue after dewaxing and protein K digestion, applying either an FFPE DNA Tissue Kit (Qiagen, Valencia, CA) or the Maxwell FFPE Tissue LEV DNA Purification Kit (Promega, Madison, WI) according to the manufacturer's protocol. Polymerase chain reaction amplifications for detecting monoclonal IGH/IGκ chain gene rearrangements were performed in selected cases according to the BIOMED-2 protocol (supplemental Methods).[28]

Fluorescence in situ hybridization

Interphase fluorescence in situ hybridization (FISH) analysis for the detection of *BCL2* and *BCL6* translocations was performed with LSI *BCL2* or *BCL6* Dual-Color Break-Apart Probes (Vysis-Abbott Molecular, Wiesbaden, Germany). In some cases, FISH for the t(14;18)/IGH/*BCL2* translocation was performed as part of the diagnostic workup.

CN analysis

DNAs extracted from FFPE were hybridized on the MIP-assay using Oncoscan FFPE according to standard protocols (Thermo Fisher Scientific, Schwerte, Germany). For comparison, previously published CN data on 35 cases of NMZL[24] and 42 of PTFL[26] were used, as well as data on t(14;18)$^+$ and t(14;18)$^-$ FL (for details see supplemental Methods).[6,7] Gains and losses and CNN-LOH regions were evaluated and visually inspected by using Nexus Biodiscovery version 9.0 software (Biodiscovery, Hawthorne, CA). Chromothripsis-like patterns were evaluated according to previously described criteria.[29] The human reference genome was GRCh37/hg19. The CNAs with a minimum size of 100 kb and CNN-LOHs larger than 5 Mb were considered informative.

NGS analysis

Next generation sequencing (NGS) analysis was performed on the Ion Torrent PGM and S5 from Thermo Fisher Scientific. NGS

libraries were amplified by using 2 primer pools of 2 Ion AmpliSeq Custom Panels covering 20 genes that have been shown to be frequently mutated in FL (panels NGS1 and NGS2; supplemental Tables 1 and 2).[2,5,30,31] The custom panels were designed with the Ion AmpliSeq Designer from Thermo Fisher Scientific (version 3.4). The library preparation, sequencing, and raw data analyses are described in the supplemental Methods.

Targeted resequencing and Sanger sequencing

For validation of the NGS results, variants with low allelic frequencies (<15%) were reanalyzed as single amplicons by using a targeted resequencing approach on the Ion Torrent PGM or S5. Variants with high allelic frequencies (≥15%) were verified with Sanger Sequencing.[26] The primer design process is described in the supplemental Methods, and the primers are shown in supplemental Tables 3 and 4.

Statistical analysis

Differences in the distribution of individual parameters among subsets of patients were analyzed by Fisher's exact test for categorized variables, and the Student *t* test for continuous variables. Nonparametric tests were applied when necessary. Details on the statistical and clustering analyses are provided in the supplemental Methods.

Results

Clinical and morphological findings

The clinical and morphological information is summarized in Table 1. A total of 55 patients were included in the study, of which 18 were men and 37 were women, representing an M/F ratio of 1:2, with a median age of 61 years (range, 33-87 years). Inguinal lymph nodes (LNs) were most frequently involved (30 of 55, 55%; isolated 20 of 50 cases, 40%), followed by axillary LNs (13 of 55; 24%), cervical LNs (8 of 55; 15%), and others (4 of 55; 7%). Of the 43 patients with available clinical information, 29 had low-stage disease at presentation (I-II; 71%); whereas 12 patients had high-stage disease (III-IV; 29%). Thirty-seven patients (86%) are alive without evidence of disease with a median follow-up of 53 months (range, 3-242 months). Nine patients showed 1 or more relapses, of which 7 are alive with no evidence of disease. Only 3 of 43 (7%) patients died of disease, 1 with transformation to diffuse large B-cell lymphoma.

Morphologically, a follicular growth pattern was observed in 33 of 55 cases (60%), a follicular and diffuse pattern in 8 of 55 cases (15%), and a predominantly diffuse pattern in 14 of 55 cases (25%) (Figure 1). Forty-eight cases (87%) were considered to have grade 1 and 2 cytology, and 7 cases (13%) were considered to have grade 3A cytology. Immunohistochemically, all cases were $CD20^+$ and/or $CD79a^+$. The GC markers BCL6 and/or CD10 were expressed in most cases (Figure 1C,J-K). CD10 was negative in 9 cases (9 of 55; 16%). BCL2 was negative in 50 cases using either the 100/D5 clone (Figure 1B,H) or the alternative clone E17 (Figure 1F,I). Five cases showed BCL2 staining. CD23 was expressed in the tumor cells in 33 of 55 cases (59%; Figure 1D,L-M). The proliferation rate showed a broad range with a median proliferation of 20% in grades 1 and 2 and 65% in grade 3A (Figure 1E).

IGH/IGκ clonality and FISH analysis

All 26 cases analyzed were monoclonal. FISH analysis demonstrated the absence of *BCL2* rearrangement in all 55 cases, using the *BCL2* break-apart probe (42 cases) and/or t(14;18) dual-color, dual-fusion probes (24 cases). *BCL6* rearrangements were identified in 10 of 45 (22%) cases.

CN and CNN-LOH alterations in $t(14;18)^-$ FL

CN-analysis of $t(14;18)^-$ FL identified 380 CNAs in 52 of 53 cases, with a mean of 7.2 imbalances per case (range, 0-28; Figure 2; supplemental Table 5). Specifically, 200 gains, 152 losses, 24 amplifications, and 4 homozygous deletions were detected. The most recurrently gained regions (≥15% of the cases) were identified at 1q21.1-q44, 2p25.3-p15/*REL&BCL11A*, 2q22.3-q36.3, 8q, 9q21.11-q34.3, 11p, 12p, and 12q. Recurrent regions of loss (≥15% of the cases) were observed at 1p36.33-p36.22/*TNFRSF14*, 6q21-q27/*TNFAIP3*, and 10q23.2-q23.31/*PTEN*. Recurrent amplifications occurred at 1q21.2-q25.3 targeting *MCL1*, *CKS1B*, and *IL6R* genes (2 cases) and 2p16.1-p15 targeting *BCL11A/REL* (2 cases). Interestingly, focal 1p36.32 homozygous deletions, including *TNFRSF14* were observed in 2 cases, whereas a single case had the 9p21.3 homozygous deletion including the *CDKN2A/B* locus. Chromothripsis-like patterns were observed in 4 cases, targeting chromosomes 1 (2 cases), 3, and 10. One hundred twenty regions of CNN-LOH were also detected, with 1p36.33-p36.11/*TNFRSF14* (26%), 16p13.3-p12.32/*CREBBP* (23%), and 6p25.3-p21.32 (15%) being the most affected regions.

Identification of recurrent mutations by targeted NGS

All cases were analyzed by NGS. The analyses of 45 cases were informative with both gene panels, whereas 9 with low DNA quality (≤200 bp) were informative only with panel 2. One case was not informative (FL23). The mean average read depth of the NGS sequence analysis was 3 551 (range, 114-26 723). In the 54 evaluable cases, 133 mutations were identified (supplemental Table 6) with a mean of 2.3 mutations per case. The most frequently mutated gene was *STAT6*, with 33 mutations in 31 patients (31 of 54; 57%) with a median variant allele frequency (VAF) of 19% (range, 4%-58%), followed by 24 *CREBBP* mutations in 22 patients (49%) with a median VAF of 25% (range, 3%-60%), 21 *TNFRSF14* mutations in 17 patients (39%) with a median VAF of 17% (range, 5%-71%), and *KMT2D* mutations in 12 patients (27%) with a median VAF of 23% (7%-44%; Figure 3; left). Additional mutated genes were *EZH2* (8 of 45; 18%), *FOXO1* (6 of 45; 13%), *HIST1H1E* (4 of 45; 9%), *TNFAIP3* (4 of 54; 7%), *EP300* (3 of 45; 7%), *HIST1H1D* (3 of 45; 7%), *SOCS1* (4 of 54; 7%), *HIST1H1C* (2 of 45; 4%), *NOTCH2* (2 of 54; 4%), *NOTCH1* (1 of 54; 2%), *MEF2B* (1 of 45; 2%), and *HIST1H1B* (1 of 45; 1%). No mutations were identified in *GNA13*, *XPO1*, *MYD88*, and *MAP2K1*.

STAT6 gene mutations were nonsynonymous and targeted the STAT6 DNA binding domain except for 1 mutation (p.R578Q) located in the SH2 domain (Figure 3; right). The most common recurrent mutation was the hot spot in amino acid residue 419 (p.D419A/G/H/N/Y) found in 17 cases (52%) followed by 4 cases (12%) each in amino acid residues 377 and 519 (p.E377K and p.D519N/V/T). *CREBBP* missense mutations were mostly identified in the HAT-KAT domain (18 mutations; 75%), whereas 6 mutations (25%) were identified in a hot spot in the zinc finger domain, causing the loss of S1680 in a 3-bp in-frame deletion,

Table 1. Clinical and morphological features of 55 patients with t(14;18)⁻ FL

Case	Sex	Age, y	Biopsy site	Cytological grading	Growth pattern	BCL2	BCL6	CD10	CD23	Ki67*, %	Stage	Clinical course
FL1	M	61	Cervical LN	1-2	Fo	−	+	+	−	20	II_{EB}	Relapse after 70 and 144 mo NED after 242 mo
FL2	F	73	Axillary LN	3A	Fo	−	+	−	−	70	NA	LFU
FL3†	M	49	Submandibular LN	1-2	Fo	−	+	+	−	25	IA	NED after 99 mo
FL4	F	50	Inguinal LN	3A	F/D	−	+	+	+	50	IA	NED after 81 mo
FL5†	F	62	Axillary LN	1-2	Fo	−	+	+	−	15	IIIA	Relapse after 43 mo NED after 150 mo
FL6	F	65	Axillary LN	1-2	Fo	−	+	+	+	15	NA	LFU
FL7	F	72	Axillary LN	1-2	Fo	−	+	+	+	10	IIIA	Relapse after 75 mo NED after 118 mo
FL8	F	53	Inguinal LN	1-2	F/D	−	+	+	+	10	IA	NED after 5 mo after that LFU
FL9	F	79	LN	1-2	Fo	−	+	−	−	10	NA	Relapse after 60 mo after that LFU
FL10	M	72	Axillary LN	1-2	D	−	+	+	+	30	IIIA	Relapse after 2, 81 and 87 mo after that LFU
FL11	F	65	Inguinal LN	1-2	F/D	−	+	+	+	30	IA	NED after 92 mo
FL12	F	79	Inguinal LN	1-2	Fo	−	+	+	−	30	IA	NED after 79 mo
FL13	F	61	LN	1-2	Fo	−	+	+	−	10	IV	No response, died with DLBCL after 10 mo
FL14	M	49	Left inguinal LN	1-2	Fo	−	+	+	+	10	II	NED after 19 mo
FL15	M	45	Inguinal LN	1-2	D	−	+	−	+	35	II	NED after 17 mo
FL16	M	60	LN	1-2	Fo	(+)	+	+	−	60	IA	NED after 12 mo
FL17	F	56	Inguinal LN	1-2	D	−	+	+	+	30	IA	NED after 8 mo
FL18†	F	65	Intraabdominal LN	1-2	Fo	−	+	+	−	20	IV	Watch and wait, no known progression after 7 mo
FL21	M	64	Right inguinal LN	1-2	F/D	−	+	+	+	10	IA	NED after 166 mo
FL22†	F	68	Cervical LN	1-2	Fo	+	+	+	−	50	IIIB	DOD (72 mo)
FL23†	M	45	Left inguinal LN	3A	Fo	(+)	+	(+)	−	40	IA	NED after 94 mo
FL24	F	50	Axillary LN	1-2	Fo	−	+	+	−	25	IIIB	NED after 189 mo
FL25	F	46	Inguinal LN	1-2	D	−	+	+	+	10	IA	NED after 41 mo
FL26	F	77	Cervical LN	1-2	Fo	−	+	−	−	15	IA	NED after 42 mo
FL27	F	79	Axillary LN	1-2	Fo	−	+	+	+	70	IA	NED after 19 mo
FL28	F	72	Right axilla LN	1-2	Fo	−	+	+	+	30	NA	NA
FL29	F	52	Left inguinal LN	1-2	F/D	−	+	+	+	30	NA	NA
FL30	M	42	Right cervical LN	3A	Fo	−	+	(+)	−	75	NA	NA
FL31	M	50	Right axilla LN	1-2	D	−	+	+	+	20	NA	NA
FL32	M	80	Inguinal LN	3A	F/D	−	(+)	−	−	30	NA	NA
FL33	F	78	Right axilla LN	1-2	Fo	−	+	+	−	20	NA	NA
FL34	M	33	Inguinal LN	1-2	F/D	−	+	+	+	30	NA	NA
FL35†	M	69	Right cervical LN	3A	Fo	−	+	−	−	60	NA	NA
FL36	F	77	Right cervical LN	1-2	Fo	−	+	+	−	20	NA	NA
FL37†	F	60	Left inguinal LN	1-2	Fo	−	+	+	+	10	IA	NED after 88 mo
FL38†	F	53	Axillary LN	1-2	Fo	−	+	+	+	30-35	II	Relapse after 48 mo NED after 63 mo
FL39	M	68	Inguinal LN	1-2	Fo	−	+	+	+	30	IA	NED after 30 mo
FL40	F	68	Axillary LN	1-2	Fo	−	+	+	−	20	IA	NED after 94 mo
FL41	F	53	Inguinal LN	1-2	F/D	−	+	+	+	20	IA	Relapse after 81 mo NED after 180 mo
FL42	F	74	Inguinal LN	1-2	Fo	−	+	+	−	80	IVA	NED after 18 mo

D, diffuse; DOD, death of disease; F, female; F/D, follicular and diffuse; Fo, follicular; LFU, lost to follow-up; M, male; NA, not available; ND, not done; NED, no evidence of disease; +, positive; (+), weakly and heterogeneously positive; −, negative.

*The median proliferation rate of grades 1 and 2 is 20% (range, 10%-90%), whereas the rate in grade 3A is 65% (range, 30%-80%).

†*BCL6* translocation.

Table 1. (continued)

Case	Sex	Age, y	Biopsy site	Cytological grading	Growth pattern	BCL2	BCL6	CD10	CD23	Ki67*, %	Stage	Clinical course
FL44	F	49	Inguinal LN	1-2	D	−	+	+	+	45	IA	NED after 24 mo
FL45	F	42	Inguinal LN	1-2	Fo	−	+	+	+	35	IA	Relapse after 24 mo NED after 48 mo
FL46	F	81	Inguinal LN	1-2	Fo	(+)	+	+	+	35	IA	NED after 24 mo
FL52†	F	76	Inguinal LN	1-2	Fo	−	+	−	+	10-15	IVA	NED after 53 mo
FL54†	M	80	Inguinal, cervical and axillary LN	3A	Fo	−	+	−	−	80	IV	Dead after 3 mo
FL57	M	46	Inguinal LN	1-2	D	−	+	+	−	20-30	IA	NED after 27 mo
FL58	F	46	Axillary LN	1-2	Fo	−	+	−	+	<10	IA	NED after 18 mo
FL59	F	87	Submandibular LN	1-2	Fo	−	+	+	+	80-90	IA	NED after 3 mo
FL60	F	49	Inguinal LN	1-2	D	−	+	+	+	10	IA	NED after 11 mo
FL62	M	61	Inguinal LN	1-2	D	−	+	+	+	15	NA	NA
FL63	F	56	Inguinal LN	1-2	D	+	+	+	+	40	III_E	NED after 109 mo
FL64	F	63	Inguinal LN	1-2	D	−	+	+	+	25	III	NED after 84 mo
FL65	M	63	Inguinal LN	1-2	D	−	+	+	+	15-20	IA	NED after 62 mo
FL66	F	51	Inguinal LN	1-2	D	−	+	+	+	20	NA	Relapse after 28 mo NED after 56 mo
FL67	F	61	Inguinal LN	1-2	D	−	+	+	+	10	IA	NED after 51 mo

D, diffuse; DOD, death of disease; F, female; F/D, follicular and diffuse; Fo, follicular; LFU, lost to follow-up; M, male; NA, not available; ND, not done; NED, no evidence of disease; +, positive; (+), weakly and heterogeneously positive; −, negative.

*The median proliferation rate of grades 1 and 2 is 20% (range, 10%-90%), whereas the rate in grade 3A is 65% (range, 30%-80%).

†*BCL6* translocation.

suggesting an important functional role for this uncharacterized serine. *TNFRSF14* mutations included 10 missense mutations, 7 nonsense mutations, 1 deletion (deletion of 3 nucleotides), and 3 frameshift mutations (insertion of 1 or 2 nucleotides). Forty-four cases (44 of 54; 81%) displayed at least 1 mutation, and 5 cases (5 of 45; 11%) showed no mutations. Sixty-two selected mutations were further verified, by either Sanger sequencing or targeted resequencing. Analysis of SIFT and Polypen 2 predicted a damaging effect in 130 of the 133 mutations (supplemental Table 6).

Three genes were frequently biallelically inactivated because of concomitant loss/CNN-LOH and mutations. Of 17 cases with *TNFRSF14* mutations, 12 were affected by local 1p36 aberrations (5 losses and 7 CNN-LOH). Of 22 cases with *CREBBP* mutations, 8 had concomitant CNN-LOH of the 16p region and 1 had a 16p loss. Finally, all 4 cases with *TNFAIP3* mutations had the 6q alteration (3 with losses and 1 with CNN-LOH).

Genetic comparison of t(14;18)$^-$ FL with cFL, NMZL, PTFL, and DTFL

The t(14;18)$^-$ FL CN profile was compared with previously published t(14;18)$^+$ and t(14;18)$^-$ FL, PTFL, and NMZL profiles.[6,7,24,26] The t(14;18)$^-$ FL in this series had more 1q21.1-q44 and 8q gains in comparison with t(14;18)$^+$ FL and more gains of 8q in comparison with other t(14;18)$^-$ cases, independent of BCL2 expression (supplemental Figure 1). In terms of CNN-LOH, only 1p36 regions were more frequently altered in t(14;18)$^-$ FL in comparison with t(14;18)$^+$ FL (26% vs 8%; $P = .004$). Compared with PTFL, t(14;18)$^-$ FL was more complex in terms of CNA (7.2 vs 0.79 alterations per case; $P < .01$; Figure 4A). t(14;18)$^-$ FL had higher genetic complexity than NMZL (7.2 vs 5.2 alterations per case; $P = .02$), but no significant differences were found. Nevertheless, gains of 18q were more frequently observed in cases of NMZL (Figure 4B).

Recurrent mutations (>5% cases) in t(14;18)$^-$ FL identified in this study were compared to previously published NGS data for t(14;18)$^+$ FL, PTFL, NMZL, and duodenal-type FL (DTFL).[5,24,25,32] This comparison showed significant differences among these entities (Figure 4C). t(14;18)$^-$ FL showed significantly more *STAT6* mutations, whereas t(14;18)$^+$ FL and DTFL had more *KMT2D* and *MEF2B* mutations. t(14;18)$^-$ FL lacked the *MAP2K1* mutations typical of PTFL, and the *NOTCH2* mutations characteristic of NMZL, whereas PTFL and NMZL had practically no *STAT6* and *CREBBP* mutations.

Genetic subgroups of t(14;18)$^-$ FL

Unsupervised cluster analysis was performed in 45 cases in which mutational analysis of all genes investigated and CNA information were available (Figure 5). Correlation with independent clinicopathological features was also performed. The unsupervised analysis recognized 2 robust molecular clusters (supplemental Figure 2). Cluster A was characterized by *TNFRSF14* mutations/1p36 alterations and mutations in other epigenetic regulators resembling cFL. In contrast, cluster B showed few genetic alterations. These 2 clusters did not distinguish cases according to inguinal localization, growth pattern, or presence of *STAT6* mutations; nevertheless, within the clusters, 4 genetic profiles were identified and designated as A1, A2, B1, and B2.

Group A1 included 15 cases and was characterized by the presence of the *TNFRSF14* mutation/1p36 CNN-LOH (100%) and frequent *STAT6* mutations (73%). Mutations in epigenetic regulator genes similar to cFL and deletions of 6q21 were mainly seen in this group. There was a female predilection (80%), with inguinal

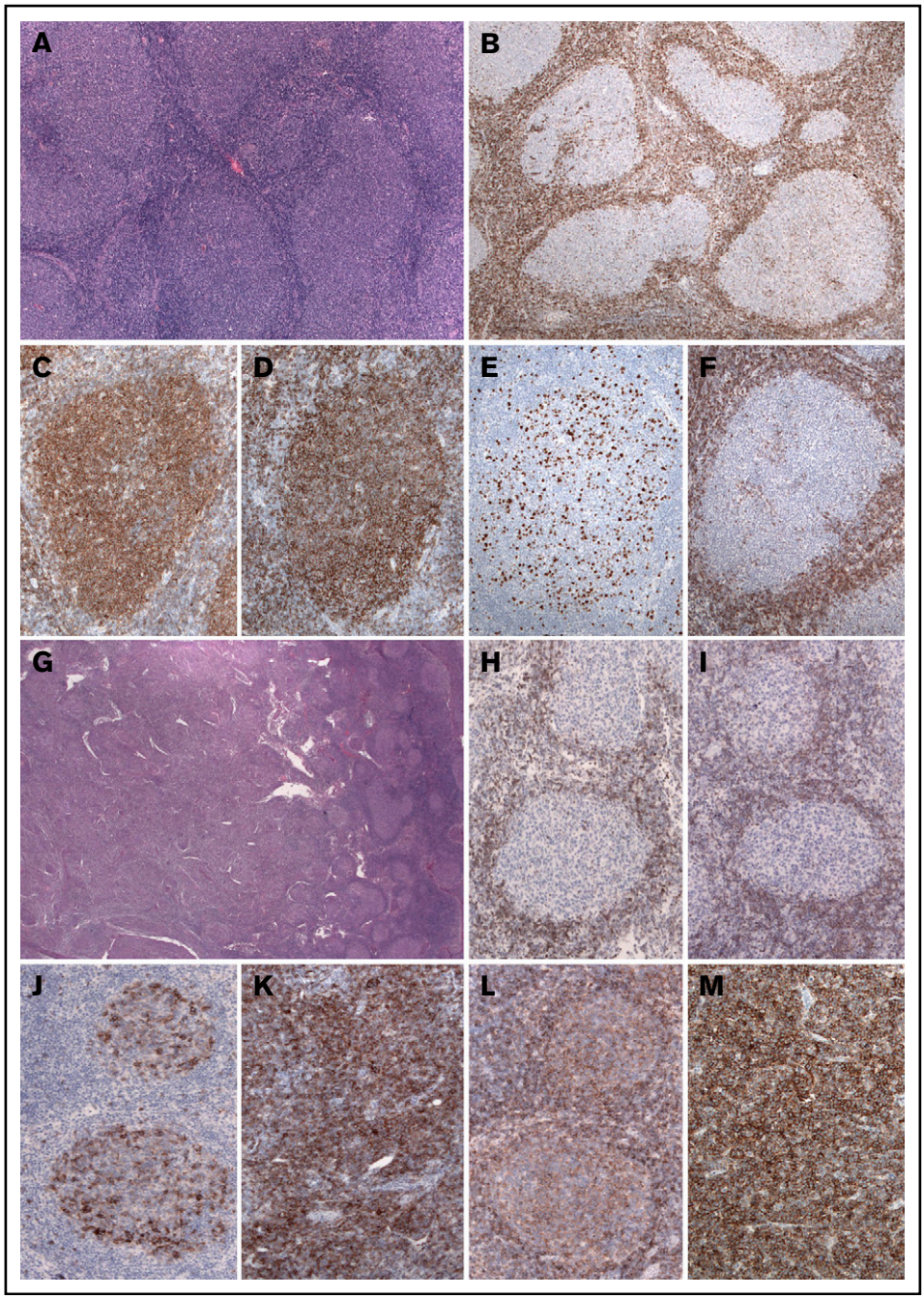

Figure 1. Histologic features of t(14;18)$^{-}$FL. (A-F) Case FL7, group B2. (A) Axillary LN with effaced architecture by an atypical lymphoid infiltration with follicular growth pattern. The follicles are back to back without well-defined mantle zones (hematoxylin and eosin [H&E]; original magnification, ×50). (B) The follicles are BCL2^{-} with the 100/D5 clone (immunoperoxidase; original magnification, ×50). (C) The follicles are CD20^{+}. (D) The tumor cells are CD23^{+}. (E) MIB1 stain demonstrates low proliferation within the follicles without polarization. (F) The tumor cells are also negative with the alternative BCL2 antibody clone E17 (C-F; immunoperoxidase; original magnification, ×100). (G-M) Case FL11, group A1. (G) Inguinal LN with atypical lymphoid proliferation with follicular (right side) and diffuse (left side) growth pattern (H&E; original magnification, ×25). (H-I) The cells are negative with the BCL2 100/D5 clone and the E17 clone. (J-K) The tumor cells are CD10^{+} in the follicular and diffuse areas. (L-M) CD23 is strongly expressed in the follicular and diffuse areas (H-M; immunoperoxidase; original magnification, ×100).

presentation in about half of the patients (53%), diffuse growth component (60%), and CD23 expression (73%). Group A2 (10 patients) was characterized by the presence of 1p36 losses (90%) with few *STAT6* mutations (30%). Inguinal presentation was seen in 50% of the patients and follicular growth pattern predominated (70%). Group B2 included 13 patients who carried *STAT6* mutations (92%) associated with *CREBBP* mutation/16p alterations (85%). These cases lacked *TNFRSF14* and *EZH2* mutations and showed few mutations in other epigenetic regulator genes, or 1p CNN-LOH and 6q deletions typical of cFL. Most patients were women presenting with disease in the inguinal region (69%), with follicular growth pattern (62%), and most often with CD23 expression (85%). Finally, group B1 (7 patients) was characterized by few genetic alterations, mainly noninguinal presentation with follicular growth pattern, lack of both *STAT6* mutations and CD23 expression ($P < .05$), and no sex predilection. There was a positive correlation between *STAT6* mutations and CD23 expression ($P = .001$).

Genetic features of patients with inguinal presentation

To further investigate the features of t(14;18)$^{-}$ FL patients with inguinal presentation, a comparative analysis was performed between patients with predominantly inguinal presentation

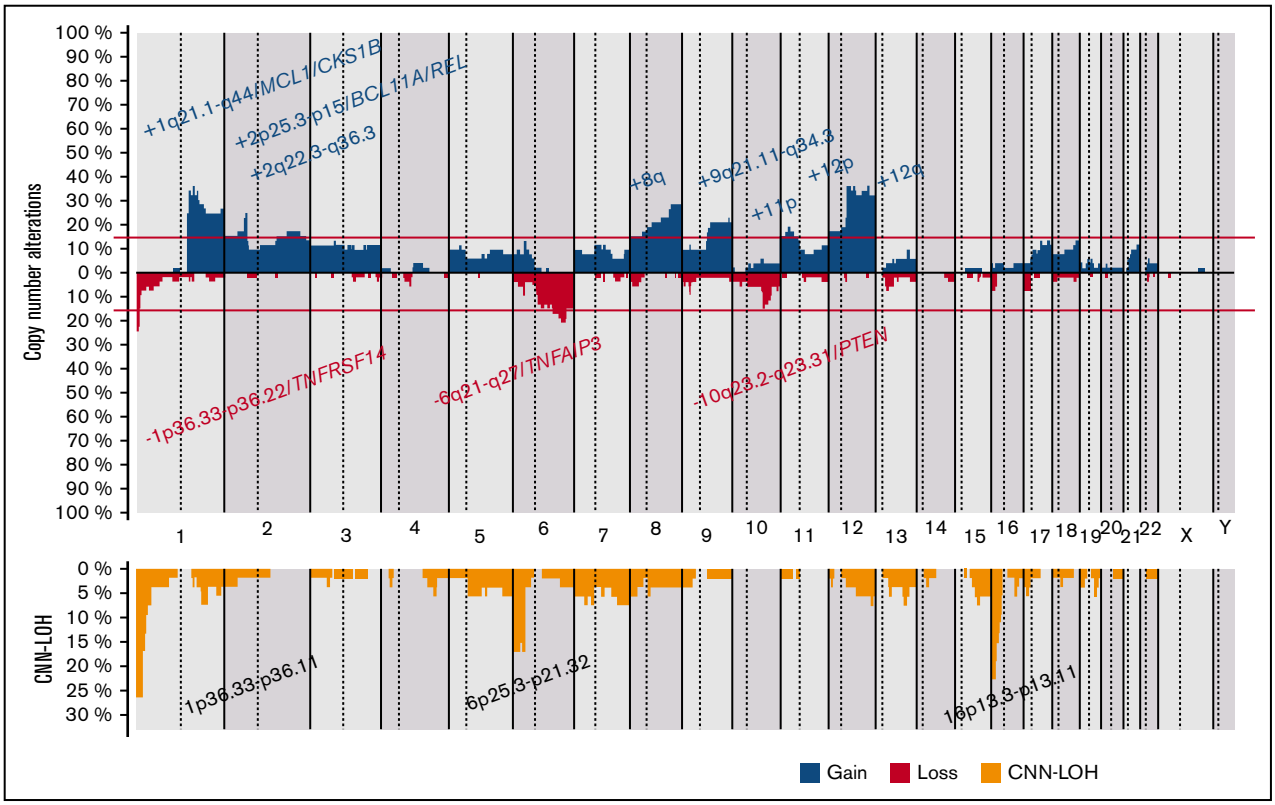

Figure 2. Copy number profile of 53 t(14;18)$^{-}$FLs. Global copy number (top panel) and copy number neutral loss of heterozygosity (CNN-LOH; bottom panel) profile. The x-axis depicts chromosome positions with dotted lines pointing out centromeres. The y-axis indicates frequency of the genomic aberration among the analyzed cases. Each probe is aligned with chromosomes from 1 to Y and p to q. Gains are depicted in blue and losses in red, and regions of CNN-LOH are represented in yellow. Recurrent CN and CNN-LOH regions (>15% of cases) are indicated.

(stage I; n = 18; stage II; n = 2) and those without inguinal presentation or inguinal stages III and IV (n = 30) (supplemental Figure 3). Patients with predominantly inguinal presentation had higher frequencies of diffuse growth component (65%), *STAT6* mutations (84%), CD23 expression (85%), and mutations in epigenetic and chromatin modifier genes (94%) and a lower number of CNAs than did patients with noninguinal or inguinal stages III and IV (5.1 vs 9.1 alterations per case); and lack of 1q gains ($P < .05$). These results were also observed when a correlation analysis of the most recurrent molecular findings (>10% of mutations and >20% of CNAs) was performed in 55 cases (supplemental Figure 4).

BCL6 rearranged t(14;18)$^{-}$ FL

Ten cases carried *BCL6* translocations with slight female predominance (male, 4; female, 6) and a median age at presentation of 64 years (range, 45-80 years). Five of 9 patients (56%) presented with advanced stage disease, in contrast to only 7 patients (24%) in the group without *BCL6* translocation ($P = .03$). All cases showed a follicular growth pattern (Figure 6): 7 were grade 1 and 2, and 3 were grade 3A. Comparison between cases with and without the *BCL6* translocation showed no significant differences in genetic complexity based on the number of CNAs (9.7 vs 7.1 alterations per case; $P = .65$). Cases with *BCL6* rearrangement more frequently carried gains of 17q than did those without. Interestingly, alterations in 17p harboring the *TP53* gene were found in 4 cases with *BCL6* rearrangement (3 with losses and 1 with CNN-LOH) but only 1 of them carried a *TP53* mutation (FL22). In contrast, only 1 case without *BCL6* rearrangement had 17p loss, without mutation. The mutational landscape was otherwise similar in cases with and without *BCL6* translocation. *BCL6*-rearranged cases did not cluster together.

Discussion

In this study, we performed a genetic analysis of the largest series of t(14;18)$^{-}$ FL reported to date, with previous studies limited by a low number of cases[6,21] or focused on cases with BCL2 expression[11] or particular morphological features.[20-22,33] We found that t(14;18)$^{-}$ FL is genetically a heterogeneous disease that is most common in women, usually presents in early clinical stages (stages I/II) at diagnosis, and has an excellent prognosis. Morphologically, cases with a pure follicular growth pattern predominated (60%), although a diffuse component was frequently observed (40%). We identified 2 molecular clusters with 4 genetic profiles that revealed key pathogenic mechanisms in t(14;18)$^{-}$ FL.

A rather characteristic finding of t(14;18)$^{-}$ FL was the high incidence of *STAT6* mutations when compared with cFL (57% vs 11%-12%; $P = .05$).[5,34] Although groups A1 and B2 shared the presence of *STAT6* mutations (23 of 28 cases; 82%), each group had unique genetic features that suggested different pathogenic mechanisms. Group A1 was the closest to cFL and included mainly cases with *TNFRSF14* mutations[35] associated with 1p36 CNN-LOH

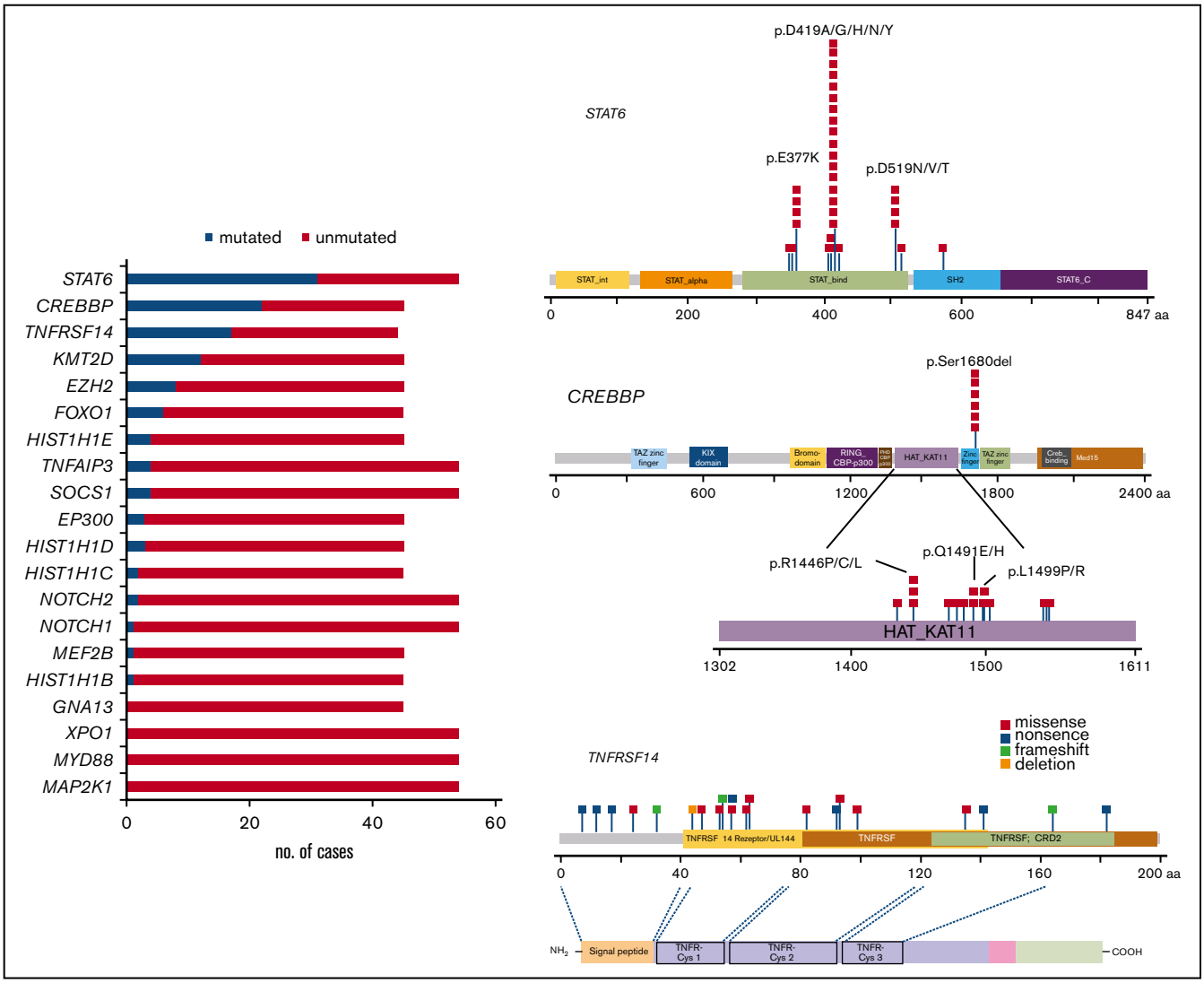

Figure 3. Mutational landscape of 54 t(14;18)⁻FLs. Bar graphs (left) show the 20 genes analyzed, and the results are given in number of mutated (blue) and nonmutated (red) cases. A diagram of the relative positions of driver mutations (right) is shown for *STAT6*, *CREBBP*, and *TNFRSF14*. The x-axis indicates the amino acid positions. The approximate location of somatic mutations identified in each gene is indicated. *STAT6* mutations are mainly in the DNA binding domain with 3 hot spots. Mutations in *CREBBP* are mainly identified in the HAT-KAT domain and a hot spot in p.S1680del. Mutations in *TNFRSF14* are identified mainly in the 3 first exons. The protein with its different domains (bottom) and the cysteine repeats TNFR-Cys 1-3. Domains of the protein are represented according to the Uniprot database (www.uniprot.org).

or deletions (71%), supporting its role as a tumor-suppressor gene.[26] In contrast to cFL, this group showed a significantly higher number of *STAT6* mutations (73% vs 11%-12%; $P < .05$) and 1p36 CNN-LOH (53% vs 8%-15%; $P < .05$). Interestingly, 1p36 deletions defined group A2; however, no correlation with *STAT6* mutations, inguinal presentation, or diffuse growth pattern was observed. Group B2, characterized by the co-occurrence of *STAT6* with *CREBBP* mutations, in the absence of *TNFRSF14* and *EZH2* mutations suggests an alternative mechanism of epigenetic "addiction." The inactivation of CREBBP alone facilitates oncogenic transformation by creating a permissive epigenetic environment in the GC that impairs the acetylation of the nonhistone proteins p53 and BCL6,[36,37] whereas activated STAT6 contributes additional survival signals. Accordingly, the co-occurrence of *STAT6* and *CREBBP* mutations has been noticed in *BCL2*⁻ and *BCL2*⁺ FL,[22,34] highlighting the cooperation of genes involved in GC fate and activated JAK-STAT signaling in the pathogenesis of some FL cases.[5,36] Nevertheless, the results of the clustering analysis must be taken cautiously, because this is a relatively small series with limited molecular information that should be confirmed in further studies.

The cases in group B1 with few genetic alterations differed from the previous groups and raised the differential diagnosis of reactive conditions or NMZL.[23,24] Nevertheless, these cases were all monoclonal: 2 cases each carried *CREBBP* mutations or *BCL6* translocations and all expressed 1 or more GC markers. Moreover, *NOTCH2* and *MYD88* mutations described in 20% and 8% to

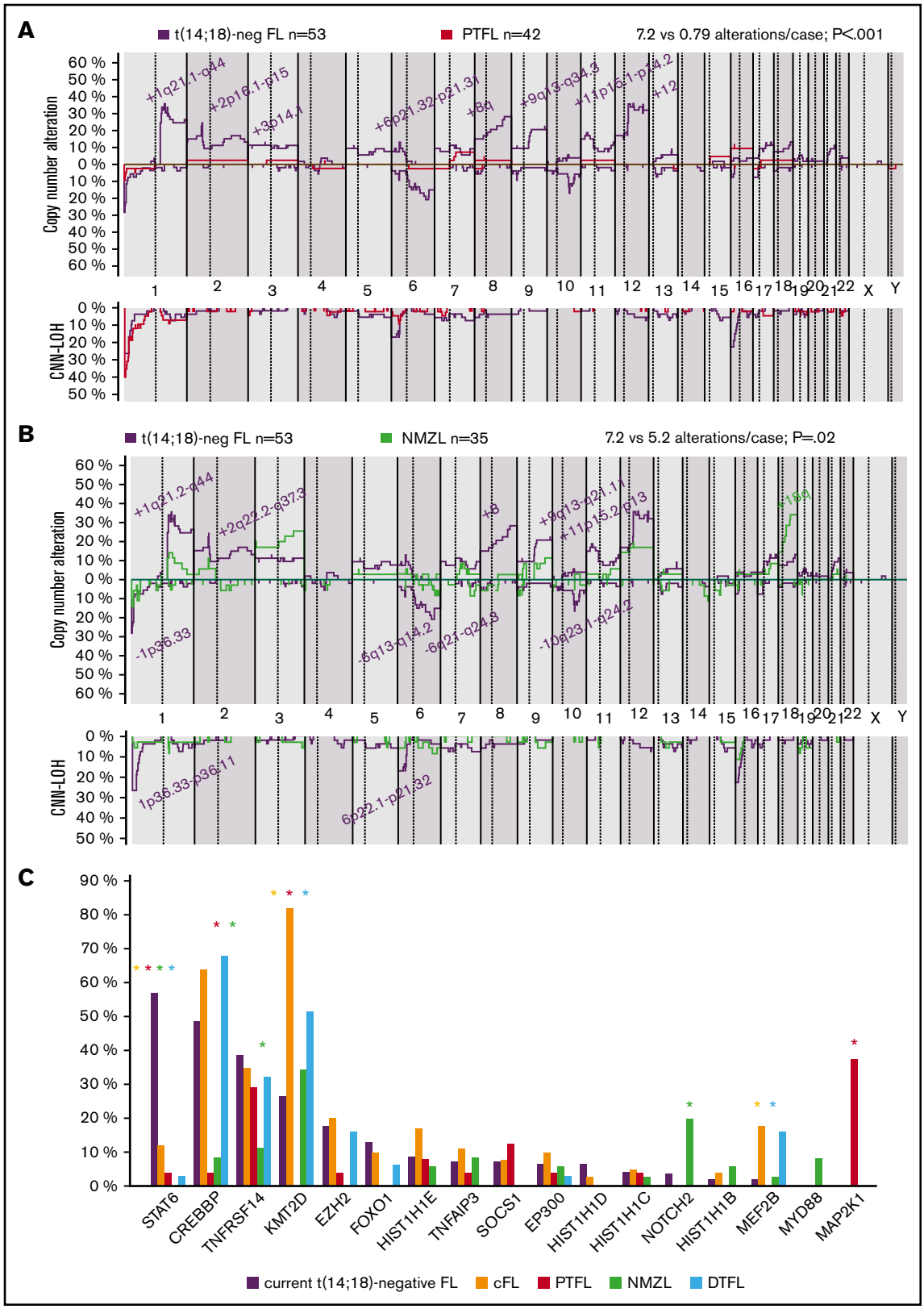

Figure 4. Genetic comparison of t(14;18)$^{-}$FL cases with cFL, PTFL, NMZL, and DTFL. (A) CN comparison of t(14;18)$^{-}$ FL vs PTFL.[26] Comparative plot of CN and CNN-LOH between 53 t(14;18)$^{-}$ FL cases and 42 PTFL cases. Significantly different regions are indicated in the plot, and the color denotes the enriched group (Fisher's exact test; adjusted $P < .05$; minimum of 3 cases). (B) CN comparison of t(14;18)$^{-}$ FL vs NMZL. Comparative plot of CN and CNN-LOH between 53 cases of t(14;18)$^{-}$ FL and 35 of NMZL. No significant differences were observed between groups (Fisher's exact test; adjusted $P < .05$; minimum of 3 cases). Nonetheless, some differences could

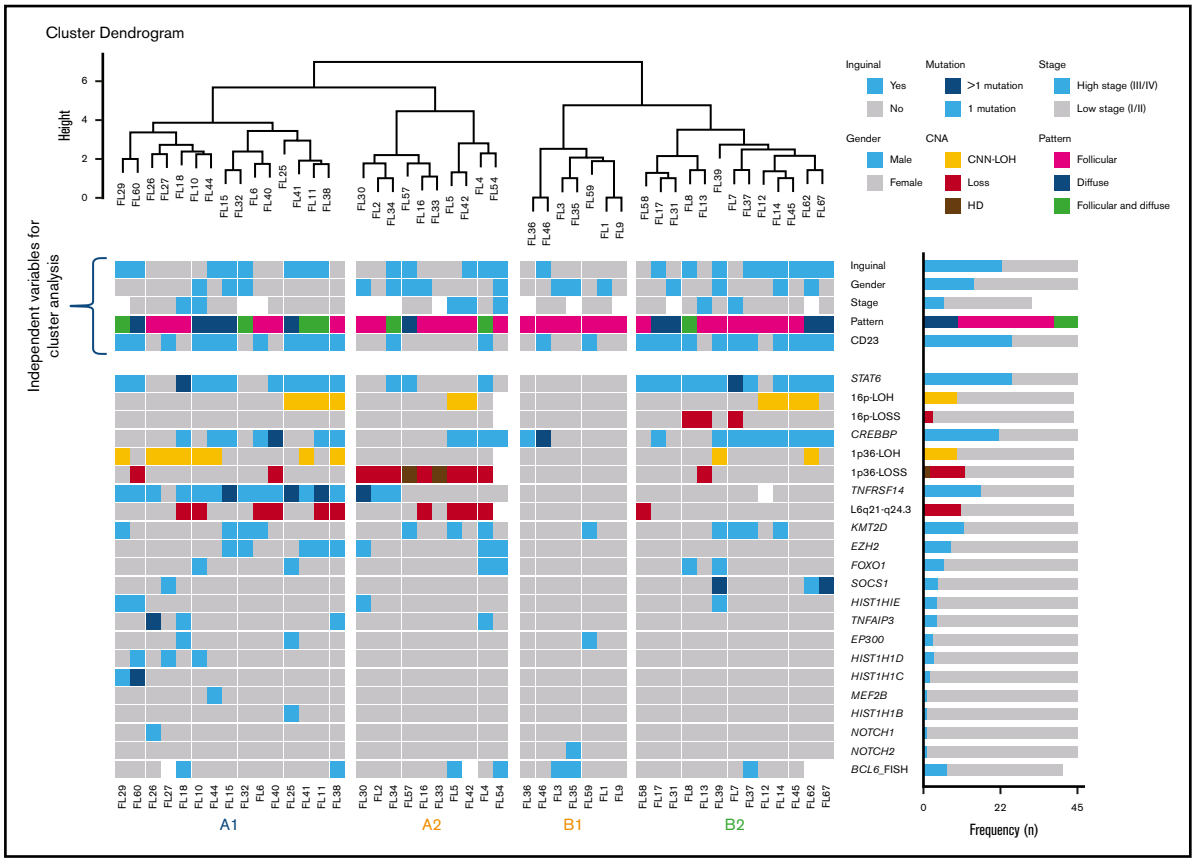

Figure 5. Cluster analysis of 45 t(14;18)$^{-}$FL cases. Only patients with complete mutational analyses were included. Independent clinical and morphological variables for cluster analysis are depicted. The cluster analysis includes NGS results and frequent CNA affecting frequently mutated gene loci. Each column represents one patient and each line one specific analysis. On the right side of the figure, the frequency of the particular result of the analysis is shown. Four identified molecular groups are labeled as A1, A2, B1, and B2.

10%, respectively in NMZL, and gains of 18q were not detected in this cohort.[24,38] Notably, cases in the B1 group as well as the other groups lack *MAP2K1* mutations characteristically found in PTFL.[25,31]

Another interesting observation in this study was the positive correlation between *STAT6* mutations and CD23 expression ($P = .001$). CD23 expression is rare in cFL but has been described as a characteristic feature of t(14;18)$^{-}$ FL.[20,21] In normal B cells the most potent inducer of CD23 is interleukin-4 (IL-4) via STAT6 activation.[39,40] In contrast, in STAT6 deficient B lymphocytes, IL-4 does not induce CD23 expression.[40] Accordingly, our data indicate that the expression of CD23 may be secondary to activating *STAT6* mutations, found to induce an exaggerated transcription of IL-4–responsive genes.[34] Importantly, the expression of CD23 in this study predicted in most cases the presence of *STAT6* mutation. Only 4 of 33 cases with CD23 expression lack demonstrable *STAT6* mutations. Interestingly, 1 of these cases (FL26) carried a *SOCS1* mutation, which is known to be upstream of STAT6 and contributes to constitutive STAT6 activation.[41-43] Therefore, the expression of CD23 may serve as a diagnostic feature that should prompt assessment of the presence of *STAT6* mutation and favors FL in the absence of t(14;18) chromosomal translocation. CD23 is usually negative in NMZL[44-46]; however, it has been reported in up to 28% of the cases in 1 study.[47] In the light of these new findings, reevaluation of previous studies of CD23^{+} NMZL cases is warranted.

An important question is whether t(14;18)$^{-}$ FL with a diffuse pattern is a distinct entity. Our results do not support this contention and demonstrate that similar genetic and clinical features can be found in t(14;18)$^{-}$ FL cases with diffuse and/or follicular growth patterns, with or without inguinal presentation. An interesting finding, however, was the lower number of CNAs ($P < .05$) in the inguinal group, which correlates well with the usually localized presentation and indolent nature of the disease. The differences observed may be attributable to the inclusion criteria used in earlier studies, which were based on t(14;18)$^{-}$ FL cases with diffuse

Figure 4. (continued) be detected using raw nonadjusted *P* values. These differentially affected regions are indicated in the plot, and the color denotes the enriched group (Fisher's exact test; $P < .05$; minimum of 3 cases).[24] (C) Comparison of recurrent mutations of t(14;18)$^{-}$ FL vs cFL, PTFL, NMZL, and DTFL. Frequencies of recurrently mutated genes (>5% cases) in 45 t(14;18)$^{-}$ cases and 22 cFL,[5] 24 PTFL,[25] 35 NMZL,[24] and 31 DTFL.[32] Asterisk color indicates significant differences between t(14;18)$^{-}$ FL and the associated color group (Fisher's exact test; $P < .05$).

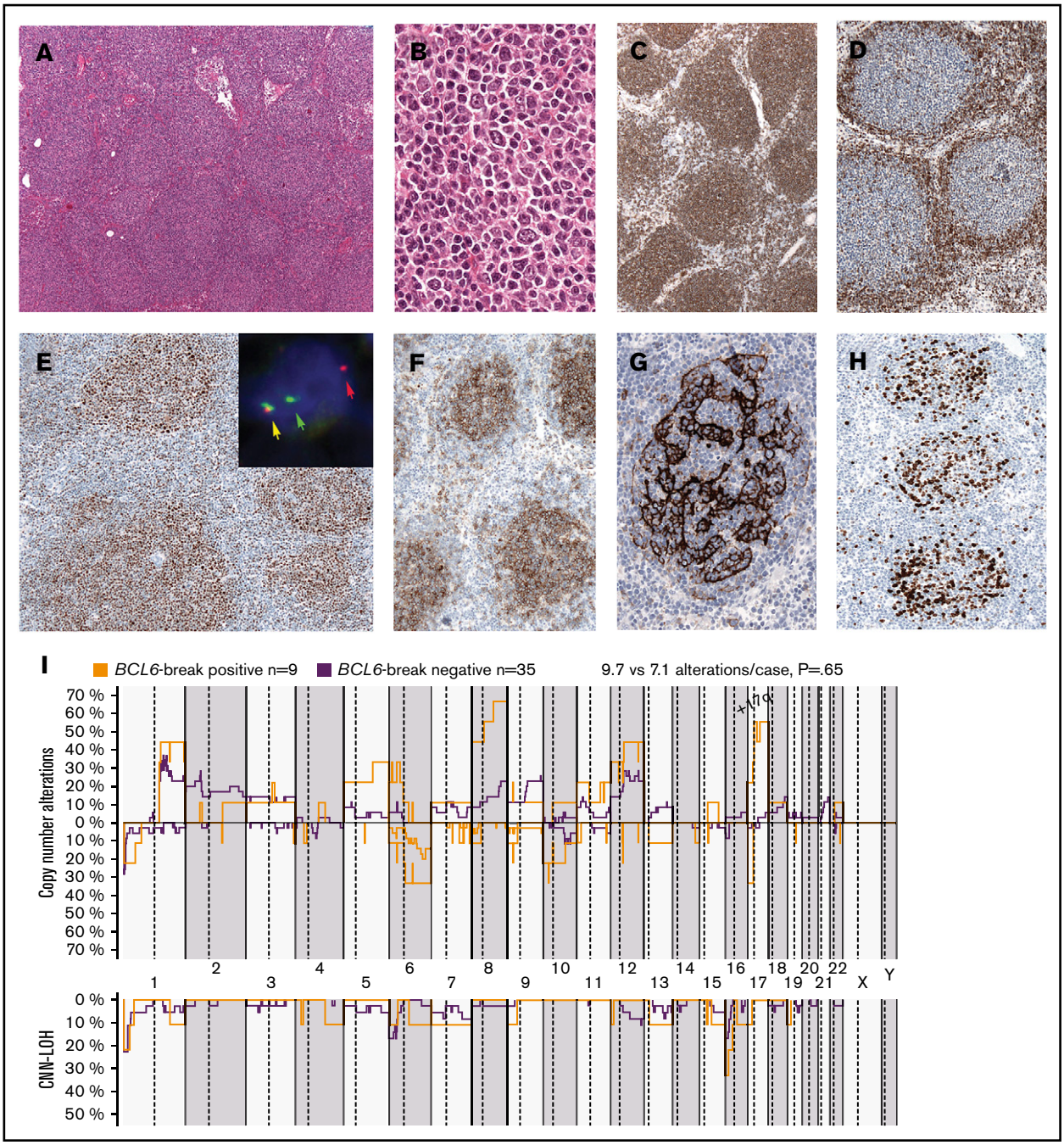

Figure 6. Morphological features and CN comparison of t(14;18)$^{-}$FL *BCL6*-break positive vs *BCL6*-break negative cases. (A-H) Case FL5, group A2. (A) Axillary LN with effaced architecture by an atypical lymphoid infiltration with follicular growth pattern. The follicles are back to back without well-defined mantle zones (hematoxylin and eosin [H&E] stain; original magnification, ×50). (B) Higher magnification demonstrates that the infiltrate is mainly composed of centrocytes with a few scattered centroblasts (H&E stain; original magnification, ×400). (C) The tumor cells are CD20^{+} (immunoperoxidase, original magnification, ×50). (D) BCL2 is negative in the tumor cells but positive in the residual mantle zones and reactive T cells. (E) The tumor cells are BCL6^{+}. FISH analysis using a *BCL6* break-apart assay (inset) shows a signal constellation of 1 colocalized signal (yellow arrow) and 1 split signal (red and green arrows) consistent with gene rearrangement. Tumor cells are CD10^{+} (F), whereas the residual follicular dendritic cells are CD23^{+} (G). Note that the tumor cells are CD23^{-}. (H) MIB1 shows a low proliferation rate without polarization in the germinal centers (D-H; immunoperoxidase; original magnification, ×100). (I) Comparative plot of CN and CNN-LOH between 9 *BCL6* break positive cases and 35 *BCL6* break negative cases. The only significantly different region is indicated in the plot, and the color denotes the enriched group (Fisher's exact test; adjusted $P < .05$; minimum 3 cases).

patterns, either alone[20,33] or with the expression of CD23[21] or the presence of 1p36 deletion.[22] In the present study, we did not preselect the cases according to morphological characteristics and included all cases with a lack of t(14;18) chromosomal alteration confirmed by FISH analysis and mostly BCL2 negativity. Another difference was the low frequency of 1p36 deletions (28%)

compared with previous studies.[20,22] This discrepancy may be explained, in part, by the various sensitivities of the technologies used in the different studies: FISH vs CN analysis.

As reported previously,[17,18] we confirmed the important role of *BCL6* in a subgroup of patients with t(14;18)$^-$ FL (22%). Patients with *BCL6* translocations, presented at more advanced clinical stages (56% vs 24%; $P = .03$) and accordingly showed a more complex genetic profile. Interestingly, in contrast to *TNFRSF14* mutated cases, *BCL6* transclocated, and *CREBBP* mutated cases were associated with a follicular growth pattern (100% and 68%, respectively), 2 master transcription regulators involved in the fate of the GC, suggesting that genetic alterations may influence the morphology of t(14;18)$^-$ FL.

Overall, t(14;18)$^-$ FL displays a typical cFL CNA profile, including aberrations of 1p/*TNFRSF14*, gains of 1q, gains of 2p16/*REL*/*BCL11A*, losses of 6q21-q24.3/*SGK1*/*TNFAIP3*, gains of 8q24/*MYC*, gains of 12q, and losses/CNN-LOH of 16p/*CREBBP* but with different frequencies. The number and the type of CNAs observed, as well as the mutational landscape in t(14;18)$^-$ FL in this study differs clearly from both NMZL and PTFL.

In summary, t(14;18)$^-$ FL is genetically a heterogeneous disorder with genetic features that differ from cFL, PTFL, and NMZL. The most distinct genetic alteration is the presence of *STAT6* mutations, which usually co-occurred with *TNFRSF14* and/or *CREBBP* alterations, revealing alternative oncogenic pathways. The genetic alterations seem to influence the morphology of t(14;18)$^-$ FL (follicular vs diffuse). Moreover, CD23 expression in t(14;18)$^-$ FL seems to be secondary to activating *STAT6* mutations. Nevertheless, there is a group of t(14;18)$^-$ FL with low genomic complexity that warrants further study.

Acknowledgements

The authors thank Sema Colak, Esther Kohler, Claudia Hermann, and Noelia Garcia for excellent technical assistance and the IDIBAPS Genomics Core Facility.

This work was supported, in part, by grants from the Deutsche Forschungsgemeinschaft (DFG; QU144/1-1 [L.Q.-M.], FE597/4-1 [F.F.], and QU144/1-1 [I.M.]), Fondo de Investigaciones Sanitarias Instituto de Salud Carlos III (Miguel Servet Program CP13/00159 and PI15/00580, [I.S.]). J.E.R.-Z. was supported by a fellowship from the Generalitat de Catalunya Agencia de Gestión de la Universidad y la Investigación (AGAUR) FI-DGR 2017 (2017 FI_B01004). E.C. is an Academia Researcher of the "Institució Catalana de Recerca I Estudis Avançats" (ICREA) of the Generalitat de Catalunya. This work was partially developed at the Centro Esther Koplowitz, Barcelona, Spain. I.S. is supported by Acció Instrumental d'Incorporació de Científics i Tecnòlegs Plan de Investigación e Innovación en Salud (PERIS) 2016 (SLT002/16/00336) from the Generalitat de Catalunya.

Authorship

Contribution: I.S. and L.Q.-M. conceived and designed the study, supervised the experimental work, analyzed the data, and wrote the manuscript; D.N. and J.E.R.-Z. performed genetic analysis, interpreted the data, and helped write the manuscript; J.E.R.-Z. and G.C. performed bioinformatics analysis; I.M., J.S., F.O., S.M., and J.S.-V. performed genetic analyses and helped interpret the data; I.B. supervised the genetic analyses and helped interpret the data; B.M. performed and interpreted the FISH analysis; D.C. performed and interpreted some clonality analyses; C.E., B.G.-F., V.S., C.L.-M., L.L., S.D., A.C., C.C.-B., F.F., E.C., E.S.J., and L.Q.-M. contributed patients, reviewed their cases, and provided clinical information; E.C., B.G.-F., O.B., E.S.J., and L.Q.-M. performed the pathological review; and E.C., E.S.J., and F.F. analyzed the data and assisted in writing the manuscript.

Conflict-of-interest disclosure: The authors declare no competing financial interests.

ORCID profiles: D.N., 0000-0002-3071-793X; J.E.R.-Z., 0000-0001-7108-7738; B.G.-F., 0000-0002-1796-7248; J.S.-V., 0000-0002-7092-9160; G.C., 0000-0003-2588-7413; D.C., 0000-0001-7486-8484; O.B., 0000-0002-5099-3675; F.F., 0000-0002-5496-293X; E.S.J., 0000-0003-4632-0301; E.C., 0000-0001-9850-9793; I.S., 0000-0002-2427-9822; L.Q.-M., 0000-0001-7156-5365.

Correspondence: Leticia Quintanilla-Martinez, Institute of Pathology, University Hospital Tübingen, Liebermeisterstr 8, 72076 Tübingen, Germany; e-mail: leticia.quintanilla-fend@med.uni-tuebingen.de; and Itziar Salaverria, Institut d´Investigacions Biomèdiques August Pi i Sunyer (IDIBAPS), Rosselló 153, 08036 Barcelona, Spain; e-mail: isalaver@clinic.cat.

References

1. Swerdlow SH, Campo E, Pileri SA, et al. The 2016 revision of the World Health Organization classification of lymphoid neoplasms. *Blood*. 2016;127(20):2375-2390.

2. Green MR, Kihira S, Liu CL, et al. Mutations in early follicular lymphoma progenitors are associated with suppressed antigen presentation. *Proc Natl Acad Sci USA*. 2015;112(10):E1116-E1125.

3. Kridel R, Sehn LH, Gascoyne RD. Pathogenesis of follicular lymphoma. *J Clin Invest*. 2012;122(10):3424-3431.

4. Loeffler M, Kreuz M, Haake A, et al; HaematoSys-Project. Genomic and epigenomic co-evolution in follicular lymphomas. *Leukemia*. 2015;29(2):456-463.

5. Okosun J, Bödör C, Wang J, et al. Integrated genomic analysis identifies recurrent mutations and evolution patterns driving the initiation and progression of follicular lymphoma. *Nat Genet*. 2014;46(2):176-181.

6. Leich E, Salaverria I, Bea S, et al. Follicular lymphomas with and without translocation t(14;18) differ in gene expression profiles and genetic alterations. *Blood*. 2009;114(4):826-834.

7. Schwaenen C, Viardot A, Berger H, et al; Molecular Mechanisms in Malignant Lymphomas Network Project of the Deutsche Krebshilfe. Microarray-based genomic profiling reveals novel genomic aberrations in follicular lymphoma which associate with patient survival and gene expression status. *Genes Chromosomes Cancer*. 2009;48(1):39-54.

8. Bouska A, Zhang W, Gong Q, et al. Combined copy number and mutation analysis identifies oncogenic pathways associated with transformation of follicular lymphoma. *Leukemia*. 2017;31(1):83-91.

9. O'Shea D, O'Riain C, Gupta M, et al. Regions of acquired uniparental disomy at diagnosis of follicular lymphoma are associated with both overall survival and risk of transformation. *Blood*. 2009;113(10):2298-2301.

10. Leich E, Hoster E, Wartenberg M, et al; German Low Grade Lymphoma Study Group (GLSG). Similar clinical features in follicular lymphomas with and without breaks in the BCL2 locus. *Leukemia*. 2016;30(4):854-860.

11. Zamò A, Pischimarov J, Schlesner M, et al. Differences between BCL2-break positive and negative follicular lymphoma unraveled by whole-exome sequencing. *Leukemia*. 2018;32(3):685-693.

12. Adam P, Baumann R, Schmidt J, et al. The BCL2 E17 and SP66 antibodies discriminate 2 immunophenotypically and genetically distinct subgroups of conventionally BCL2-"negative" grade 1/2 follicular lymphomas. *Hum Pathol*. 2013;44(9):1817-1826.

13. Leich E, Zamo A, Horn H, et al. MicroRNA profiles of t(14;18)-negative follicular lymphoma support a late germinal center B-cell phenotype. *Blood*. 2011; 118(20):5550-5558.

14. Baron BW, Billstrand C, Madronero L, McKeithan TW. *Hin*dIII polymorphism in the BCL6 gene. *Hum Mol Genet*. 1993;2(9):1513.

15. Horn H, Schmelter C, Leich E, et al. Follicular lymphoma grade 3B is a distinct neoplasm according to cytogenetic and immunohistochemical profiles. *Haematologica*. 2011;96(9):1327-1334.

16. Ott G, Katzenberger T, Lohr A, et al. Cytomorphologic, immunohistochemical, and cytogenetic profiles of follicular lymphoma: 2 types of follicular lymphoma grade 3. *Blood*. 2002;99(10):3806-3812.

17. Horsman DE, Okamoto I, Ludkovski O, et al. Follicular lymphoma lacking the t(14;18)(q32;q21): identification of two disease subtypes. *Br J Haematol*. 2003;120(3):424-433.

18. Jardin F, Gaulard P, Buchonnet G, et al. Follicular lymphoma without t(14;18) and with BCL-6 rearrangement: a lymphoma subtype with distinct pathological, molecular and clinical characteristics. *Leukemia*. 2002;16(11):2309-2317.

19. Gu K, Fu K, Jain S, et al. t(14;18)-negative follicular lymphomas are associated with a high frequency of BCL6 rearrangement at the alternative breakpoint region. *Mod Pathol*. 2009;22(9):1251-1257.

20. Katzenberger T, Kalla J, Leich E, et al. A distinctive subtype of t(14;18)-negative nodal follicular non-Hodgkin lymphoma characterized by a predominantly diffuse growth pattern and deletions in the chromosomal region 1p36. *Blood*. 2009;113(5):1053-1061.

21. Siddiqi IN, Friedman J, Barry-Holson KQ, et al. Characterization of a variant of t(14;18) negative nodal diffuse follicular lymphoma with CD23 expression, 1p36/TNFRSF14 abnormalities, and STAT6 mutations. *Mod Pathol*. 2016;29(6):570-581.

22. Zamò A, Pischimarov J, Horn H, Ott G, Rosenwald A, Leich E. The exomic landscape of t(14;18)-negative diffuse follicular lymphoma with 1p36 deletion. *Br J Haematol*. 2018;180(3):391-394.

23. van den Brand M, van der Velden WJ, Diets IJ, et al. Clinical features of patients with nodal marginal zone lymphoma compared to follicular lymphoma: similar presentation, but differences in prognostic factors and rate of transformation. *Leuk Lymphoma*. 2016;57(7):1649-1656.

24. Spina V, Khiabanian H, Messina M, et al. The genetics of nodal marginal zone lymphoma. *Blood*. 2016;128(10):1362-1373.

25. Louissaint A Jr., Schafernak KT, Geyer JT, et al. Pediatric-type nodal follicular lymphoma: a biologically distinct lymphoma with frequent MAPK pathway mutations. *Blood*. 2016;128(8):1093-1100.

26. Schmidt J, Gong S, Marafioti T, et al. Genome-wide analysis of pediatric-type follicular lymphoma reveals low genetic complexity and recurrent alterations of TNFRSF14 gene. *Blood*. 2016;128(8):1101-1111.

27. Quintanilla-Martinez L, Sander B, Chan JK, et al. Indolent lymphomas in the pediatric population: follicular lymphoma, IRF4/MUM1+ lymphoma, nodal marginal zone lymphoma and chronic lymphocytic leukemia. *Virchows Arch*. 2016;468(2):141-157.

28. van Dongen JJ, Langerak AW, Brüggemann M, et al. Design and standardization of PCR primers and protocols for detection of clonal immunoglobulin and T-cell receptor gene recombinations in suspect lymphoproliferations: report of the BIOMED-2 Concerted Action BMH4-CT98-3936. *Leukemia*. 2003; 17(12):2257-2317.

29. Edelmann J, Holzmann K, Miller F, et al. High-resolution genomic profiling of chronic lymphocytic leukemia reveals new recurrent genomic alterations. *Blood*. 2012;120(24):4783-4794.

30. Karube K, Martínez D, Royo C, et al. Recurrent mutations of NOTCH genes in follicular lymphoma identify a distinctive subset of tumours. *J Pathol*. 2014; 234(3):423-430.

31. Schmidt J, Ramis-Zaldivar JE. Mutations of MAP2K1 are frequent in pediatric-type follicular lymphoma and result in ERK pathway activation. *Blood*. 2017; 130:323-327.

32. Hellmuth JC, Louissaint A Jr., Szczepanowski M, et al. Duodenal-type and nodal follicular lymphomas differ by their immune microenvironment rather than their mutation profiles. *Blood*. 2018;132(16):1695-1702.

33. Xian RR, Xie Y, Haley LM, et al. CREBBP and STAT6 co-mutation and 16p13 and 1p36 loss define the t(14;18)-negative diffuse variant of follicular lymphoma. *Blood Cancer J*. 2020;10(6):69.

34. Yildiz M, Li H, Bernard D, et al. Activating STAT6 mutations in follicular lymphoma. *Blood*. 2015;125(4):668-679.

35. Boice M, Salloum D, Mourcin F, et al. Loss of the HVEM Tumor Suppressor in Lymphoma and Restoration by Modified CAR-T Cells. *Cell*. 2016;167: 405-418 e13.

36. Zhang J, Vlasevska S, Wells VA, et al. The CREBBP Acetyltransferase Is a Haploinsufficient Tumor Suppressor in B-cell Lymphoma. *Cancer Discov*. 2017;7(3):322-337.

37. Meyer SN, Scuoppo C, Vlasevska S, et al. Unique and Shared Epigenetic Programs of the CREBBP and EP300 Acetyltransferases in Germinal Center B Cells Reveal Targetable Dependencies in Lymphoma. *Immunity*. 2019;51:535-47 e9.

38. Swerdlow SH, Kuzu I, Dogan A, et al. The many faces of small B cell lymphomas with plasmacytic differentiation and the contribution of MYD88 testing. *Virchows Arch*. 2016;468(3):259-275.

39. Takeda K, Kishimoto T, Akira S. STAT6: its role in interleukin 4-mediated biological functions. *J Mol Med (Berl)*. 1997;75(5):317-326.

40. Takeda K, Tanaka T, Shi W, et al. Essential role of Stat6 in IL-4 signalling. *Nature*. 1996;380(6575):627-630.

41. Ritz O, Guiter C, Dorsch K, et al. STAT6 activity is regulated by SOCS-1 and modulates BCL-XL expression in primary mediastinal B-cell lymphoma. *Leukemia*. 2008;22(11):2106-2110.

42. Mottok A, Renné C, Seifert M, et al. Inactivating SOCS1 mutations are caused by aberrant somatic hypermutation and restricted to a subset of B-cell lymphoma entities. *Blood*. 2009;114(20):4503-4506.

43. Mottok A, Renné C, Willenbrock K, Hansmann ML, Bräuninger A. Somatic hypermutation of SOCS1 in lymphocyte-predominant Hodgkin lymphoma is accompanied by high JAK2 expression and activation of STAT6. *Blood*. 2007;110(9):3387-3390.

44. van den Brand M, van Krieken JH. Recognizing nodal marginal zone lymphoma: recent advances and pitfalls. A systematic review. *Haematologica*. 2013; 98(7):1003-1013.

45. Traverse-Glehen A, Felman P, Callet-Bauchu E, et al. A clinicopathological study of nodal marginal zone B-cell lymphoma. A report on 21 cases. *Histopathology*. 2006;48(2):162-173.

46. Campo E, Miquel R, Krenacs L, Sorbara L, Raffeld M, Jaffe ES. Primary nodal marginal zone lymphomas of splenic and MALT type. *Am J Surg Pathol*. 1999;23(1):59-68.

47. Naresh KN. Nodal marginal zone B-cell lymphoma with prominent follicular colonization - difficulties in diagnosis: a study of 15 cases. *Histopathology*. 2008;52(3):331-339.